Decadal Variations in the Global Atmospheric Land Temperatures

Richard A. Muller[1,2,3], Judith Curry[4], Donald Groom[2], Robert Jacobsen[1,2], Saul Perlmutter[1,2], Robert Rohde[3], Arthur Rosenfeld[1,2], Charlotte Wickham[5], Jonathan Wurtele[1,2]

[1] Dept. of Physics, University of California, Berkeley CA 94720; [2]Lawrence Berkeley National Laboratory, Berkeley CA 94720; [3]Novim Group, Berkeley Earth Surface Temperature Project, 211 Rametto Road, Santa Barbara CA 92104 ; [4]Georgia Institute of Technology, Atlanta GA 30332; [5]University of California, Berkeley, now at Dept. of Statistics, Oregon State University. Correspondence for all authors should be sent to The Berkeley Earth Surface Temperature Project, 2831 Garber St., Berkeley CA 94705.

Abstract

Interannual to decadal variations in Earth global temperature estimates have often been identified with El Nino Southern Oscillation (ENSO) events. However, we show that variability on timescales of 2-15 years in mean annual global land surface temperature anomalies, Tavg are more closely correlated with variability in sea surface temperatures in the North Atlantic. In particular, the cross-correlation of annually-averaged values of Tavg with annual values of the AMO, the Atlantic Mutidecadal Oscillation index, is much stronger than the cross-correlation of Tavg with ENSO. The pattern of fluctuations in Tavg from 1950 to 2010 reflects true climate variability, and is not an artifact of station sampling. A world map of temperature correlations shows that the association with AMO is broadly distributed and unidirectional. The effect of El Nino on temperature is locally stronger, but can be of either sign, leading to less impact on the global average. We identify one strong narrow spectral peak in the AMO at period 9.1 ± 0.4 years and p-value 1.7% (CL 98.3%). Variations in the flow of the Atlantic Meridional Overturning Circulation may be responsible for some of the 2-15 year variability observed in global land temperatures.

1. Introduction

The average earth land surface temperature, Tavg, is a key indicator of climate change. Detailed analyses of Tavg have been reported by three major teams: the National Oceanographic and Atmospheric Administration (NOAA; see Menne et al. [2005]), the NASA Goddard Institute for Space Science (GISS; see Hansen et al. [2010]), and a collaboration of the Hadley Centre of the UK Meteorological Office with the Climate Research Unit of East Anglia (HadCRU; see Jones et al. [2003], Brohan et al. [2005]). Results from their analysis are shown in Figure 1. The time period in the plot begins at 1950 since a large number of new stations were introduced at that time. The uncertainties prior to 1950 are substantially larger. Note that in this paper we focus of the land-only temperature average – not including oceans – so that the time series will not directly include the ocean data that we will use for our correlation analysis.

Also shown in Figure 1 is a new estimate of the Earth atmospheric land surface temperature that we created from data independent of that used by the other three groups. We obtained this estimate by choosing 2000 sites randomly from a list of approximately 30,964 temperature recording stations world-wide that had not been used by NOAA, GISS, or HadCRU. Each temperature record was adjusted by an additive parameter, one per record, to bring it into a best least-squares fit with the other records; details of this procedure are described by Rohde et al. [2011]. The statistical techniques used (Kriging) are designed to compensate for sampling biases in station coverage. This permits a random selection of stations to be made without giving excessive weight to heavily sampled regions, such as North America and Europe. No adjustments or corrections were made for systematic effects such as urban heat island warming or change of instrumentation. Despite these limitations,

the virtue of this estimate is that it is derived independently from previously used data. Because of this, the qualitative agreement with the prior estimates confirms that the fluctuations are true indicators of climate and not artifacts of data selection and processing. The four curves show a broad trend of "global warming" with some unevenness; the lack of warming from 1950 to 1975 has been attributed to a combination of natural and anthropogenic factors, especially the cooling effect of increased aerosol pollution [Jones et al., 2003].
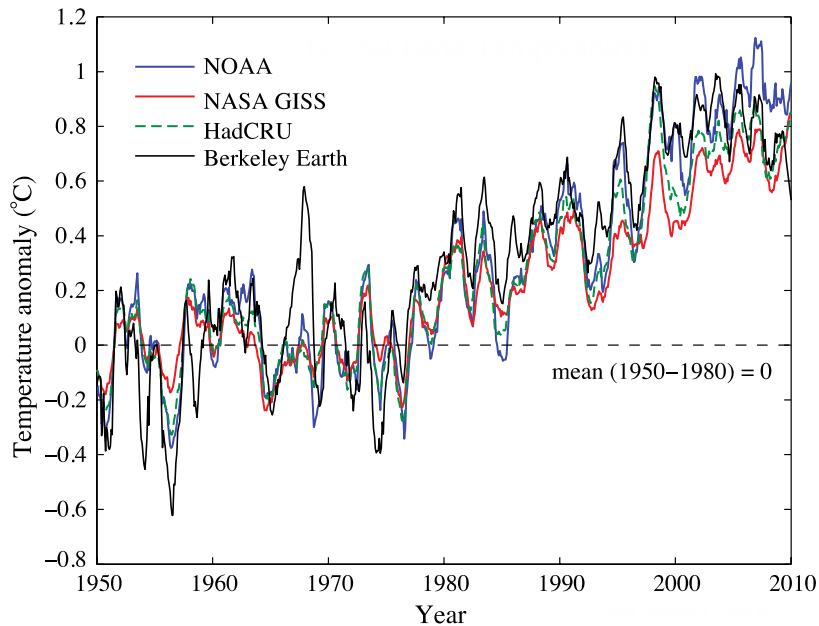

Figure 1. Global land temperature estimates Tavg, smoothed by a 12-month moving average. The temperature anomaly is the difference between the estimated temperature and the mean in the period 1950-1980 for each temperature series. Note the similarity of many of the short-term fluctuations with periods 2-15 years. The Berkeley Earth data were randomly chosen from 30,964 sites that were not used by the other groups.

2. Decadal (2 – 15 yr) Variations

Much attention has been given to the small Tavg maxima of 1998 and 2005. The maximum in 1998 occurred during a very strong El Nino, and is plausibly associated with that oceanic event [Trenberth, 2002]. In this study we examined the annually-averaged global land temperature time series to study their possible correlation not only with the El Nino Southern Oscillation index (ENSO; see NOAA [2005]) but with the Atlantic Multidecadal Oscillation (AMO; see Schlesinger et al. [1994] and Enfield et al. [2001]), the Pacific Decadal Oscillation (PDO, see Zhang et al. [1997]), the North Atlantic Oscillation (NAO, see Zhang et al. [1997], Hurrell et al. [1995]), and the Arctic Oscillation (AO, see Thompson et al. [1998]). Three of these indices: ENSO, AMO, PDO, are derived from sea surface temperature records, in the equatorial Pacific, the North Atlantic, and the North Pacific respectively. Two of these, the NAO and the AO, are derived from surface pressure differences at locations in the northern Atlantic and

Arctic. We find that the strongest cross-correlation of the decadal fluctuations in land surface temperature is not with ENSO but with the AMO. The AMO index is plotted in Figure 2.
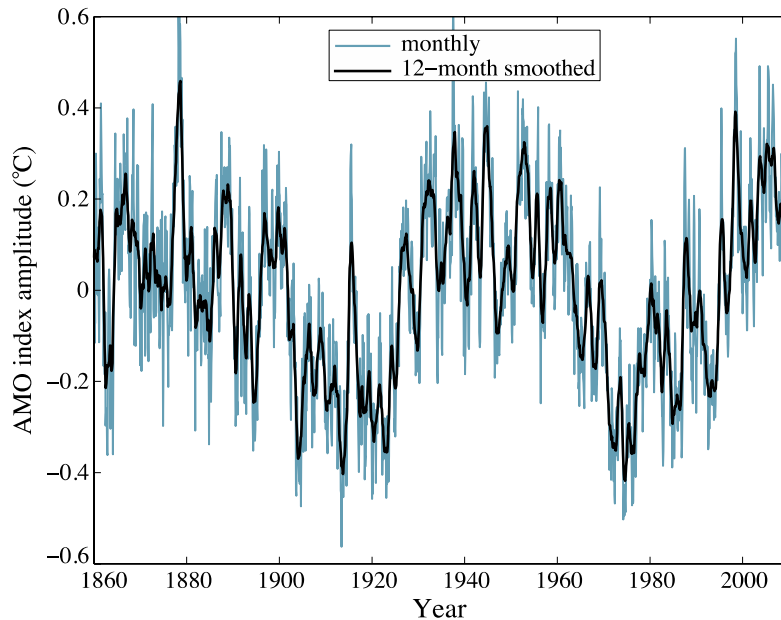

Figure 2. The AMO index. The pattern is dominated by the 65-70 year multidecadal oscillation that gave the index its name. In this paper, we are more interested in the short-term 2-15 year variations that are evident in the 12-month smoothed curve.

Our analysis used the monthly land-surface average temperature records made available by the four groups previously referenced: NOAA, NASA GISS, HadCRU, and ours, the Berkeley Earth Surface Temperature group. The land temperature data were smoothed with a 12-month running average (boxcar smoothing); this removes high frequency (e.g. monthly) changes. The data prior to 1950 were noisier than the subsequent data, primarily because the number of stations was smaller, and for that reason we restricted the period for our analysis to 1950-2010.

To emphasize the decadal-scale variations, the long-term changes in the temperature records and oceanic indices were "pre-whitened." This is a process to remove a large signal that is not being studied in order to reduce bias in the remainder. To do this, we fit each record (yearly data sets) separately to 5th order polynomials using a linear least-squares regression; we subtracted the respective fits, and normalized the results to unit mean-square deviation. This procedure effectively removes slow changes such as global warming and the ~70 year cycle of the AMO, and gives each record zero mean. The 12-month smoothing removes high frequency (e.g. monthly) changes. All of the remaining analysis in this paper is based on the pre-whitened temperature records and oceanic indices.

The four temperature estimates after this conditioning are shown in Figure 3A. In 3B and 3C, these four temperature estimates were averaged and compared, in turn, to the

conditioned AMO and ENSO. In 3C we directly compare the AMO and ENSO decadal variations.
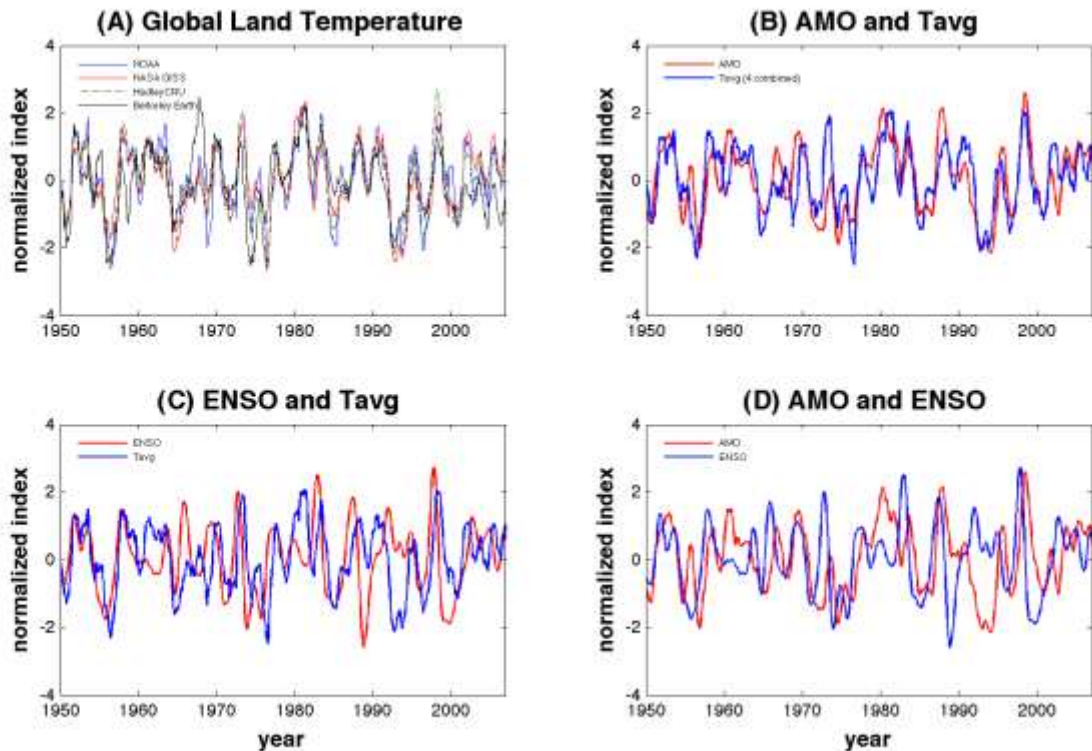

Figure 3. Decadal fluctuations in surface land temperature estimates and in oceanic indices. The long-term variability was suppressed by removing the least-squares fit 5th order polynomial from each curve. (A) shows the 12-month smoothed land surface temperature estimates from the four groups. The decadal variations are very similar to each other. The Berkeley Earth data were derived from 2000 sites chosen randomly from a set of 30964 that did not include any of the sites from the other groups. (B) shows the AMO index compared to Tavg, the average of the four land estimates. (C) shows the ENSO index compared to the average of the four land estimates. (D) shows the AMO and ENSO directly. Note that the AMO agreement in (b) is qualitatively stronger than the ENSO agreement in (c).

3. Difference and Correlation Analysis

Visual inspection of Figure 3 suggests that the AMO fluctuations match the temperature variations better than does the ENSO index almost everywhere; perhaps the only prominent exception being 1968 – 1973. This impression is verified by calculating the RMS (root-mean-squared) differences of pairs of plots. The results are shown in Table 1. Note that the RMS of the difference between ENSO and Tavg is over 50% larger than the RMS of the difference between AMO and Tavg. The RMS of the difference between AMO and ENSO is 67% larger than that of AMO and Tavg. The "random" signal, put to show the RMS expected when there is no correlation, was

created by breaking the ENSO signal into 10 parts and randomly scrambling them; the RMS of the difference between it and the AMO agrees with the theoretical expectation of √2.

records	RMS
(4 estimates) – Tavg	0.26 C
AMO – Tavg	0.75 C
ENSO – Tavg	1.14 C
AMO – ENSO	1.25 C
AMO - random	1.41 C

Table 1. Root-mean-squared difference of the data shown in Figure 3. The first row shows the RMS deviation of the 4 temperature estimates from Tavg, the average of the four. The other entries show the RMS deviation of the signal differences. The "random" signal was generated by breaking ENSO into 10 parts and randomly scrambling them in time.

To quantify further the relationship between Tavg and AMO and ENSO, we performed a correlation analysis. Correlation C(A ,B) is a measure of the linear time invariant dependence between two time series {A(t)} and {B(t)}. Here, A and B represent either pre-whitened temperature signals or oceanic indices, normalized to zero mean and unit standard deviation. If we include the possibility of a time delay or lag L between the two signals, then we can define the cross-correlation C as

$$(A, B; L) = \frac{1}{N(L)} \sum A(t)B(t + L)$$

where A and B have zero mean and unit standard deviation and N(L) is the number of terms in the sum. With this definition, the correlation of a function can vary between –1 and +1. At zero lag, the autocorrelation = 1. The value of the correlation at zero lag is commonly called Pearson's Correlation Coefficient, often designated by r.

The correlation estimates between major temperature records and oceanic indices are shown in Figure 4. In these plots, a peak at 0 lag indicates a direct linear correlation between the data sets. A peak offset from zero also indicates correlation but with one lagging the other by the offset.
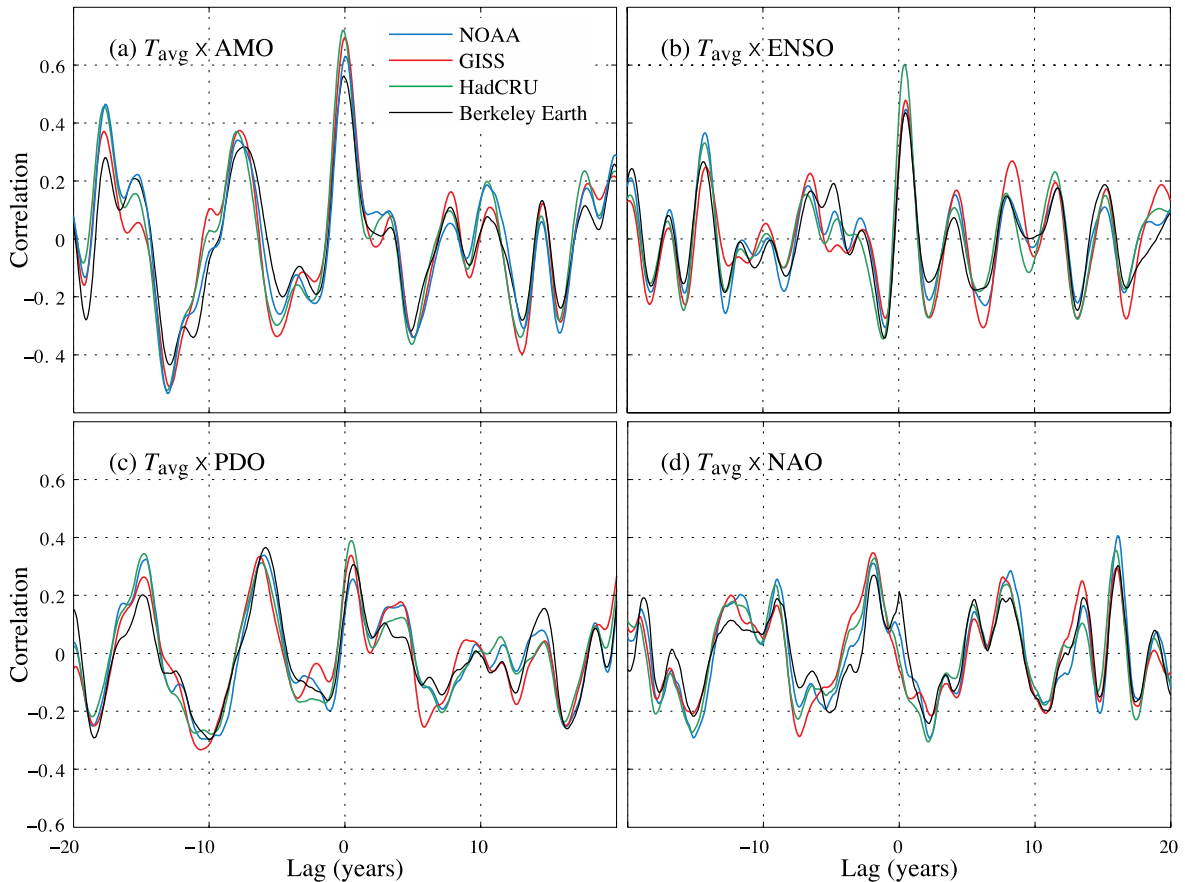
Figure 4 . Decadal correlations of the Berkeley Earth land temperature estimates Tavg with the (a) AMO index, (b) ENSO index, (c) PDO index, and (d) NAO index. The strongest correlation observed, 0.65 ± 0.04, is with the AMO.

The strongest correlation is observed between the estimates of the average land temperature Tavg and AMO, the Atlantic Multidecadal oscillation, with a correlation coefficient r = 0.65 ± 0.04. (In this paper, ± refers to 1 standard error, frequently called by physicists "one standard deviation".) This is the highest peak in any of the cross-correlation plots we calculated, and it occurs at zero lag. The correlation coefficient for the temperature data with ENSO is substantially less, with r = 0.49 ± 0.04. The error uncertainties were estimated from the variance of the four correlations. There is no statistically significant correlation seen in panels (c) and (d).

For reference, the maximum correlation between AMO and ENSO in these data is 0.50 ± 0.04; with AMO lagging ENSO by 0.70 ± 0.25 years. This is a somewhat larger lag than previously reported in a more detailed analysis of ENSO by Trenberth et al. [2002].

To estimate the statistical significance of the AMO r-factor, we did a permutation test based on a Monte-Carlo simulation. The AMO pre-whitened record contains 16 points at which the index rises through zero; we chopped the record at these points, creating 17 AMO segments. The order of these segments was then permuted randomly and reassembled, creating a simulated AMO. Because of the manner of cutting, the

scrambled AMO has many of the same statistical properties as the original AMO; it has the identical amplitude distribution as well as the same number and shapes of peaks and valleys; indeed, it looks to the eye very much like the original AMO. We generated 1,000,000 of these simulated AMOs, and calculated the correlation coefficient r for each of these with the Tavg of the Berkeley Earth surface land temperature record. In those 1,000,000 simulated AMO trials, the highest value of r obtained was 0.49, substantially less than the value of 0.65 ± 0.04 obtained with the real AMO, giving a p-factor less than 10-6. Of course, it is not too surprising that land temperature estimates are correlated with sea temperature indices; the key observation is that for interannual to decadal variations, it is the AMO that has the strongest correlation, not ENSO or one of the other indices.

Figure 5(A) shows the conditioned AMO and PDO indices as a function of time. It can be seen on this plot that PDO generally leads AMO. The correlation is shown in Figure 5(B). Although the correlation peaks near zero lag, the bulk of the central correlation peak is at a lag of about 2 years. The periodicity of the correlation plot is an indication of a periodicity in both AMO and PDO that we will discuss next.
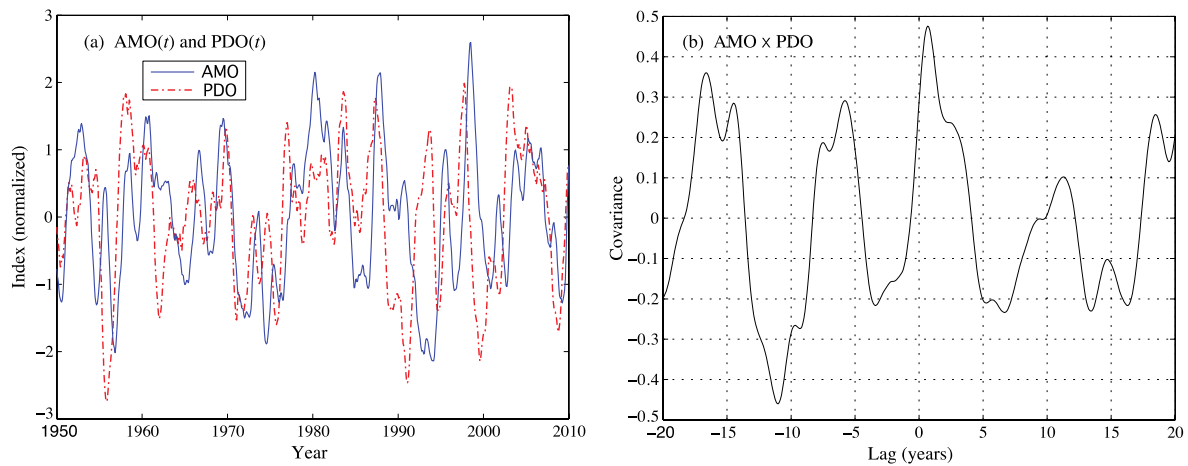

Figure 5. (a) shows the pre-whitened AMO and PDO indices plotted together vs time. It can be seen that PDO leads AMO by about 2.5 years. (b) shows the correlation of AMO and PDO vs lag. The periodicity of the correlation (4.5 cycles in 40 years of lag) is a result of the apparent presence of a 9-year cycle in both.

It is not possible from the correlations to ascribe causality with any certainty. For example, Zhang and Delworth [2007] suggested that the observed AMO leads the inverted PDO index by about 12 years, and discussed the possible mechanism for the Atlantic-Pacific linkage. On our plot Figure 5(b) this corresponds to the large downward variation at Lag of negative 12 years. Such ambiguities could be addressed by mapping the correlation over the world as a function of time.

4. Correlation Map

In Figure 6 we show a map of the decadal correlations of both AMO and ENSO with the NOAA global temperature anomaly map; this map includes oceans as well as land.

The association with AMO is broadly distributed and unidirectional. The effect of El Nino on temperature is locally stronger, but can be of either sign, leading to less impact on the global average. The strong correlation of AMO with the Atlantic is, of course, a result of the fact that the AMO is derived from Atlantic temperatures; similarly for the strong correlation between ENSO and the equatorial Pacific. ENSO also shows a strong correlation with the Indian ocean. On the land, the AMO affects Africa, southern Asia, and Canada; ENSO correlates most strongly to the continents in the Southern hemisphere. Note its weak correlation to the Atlantic.
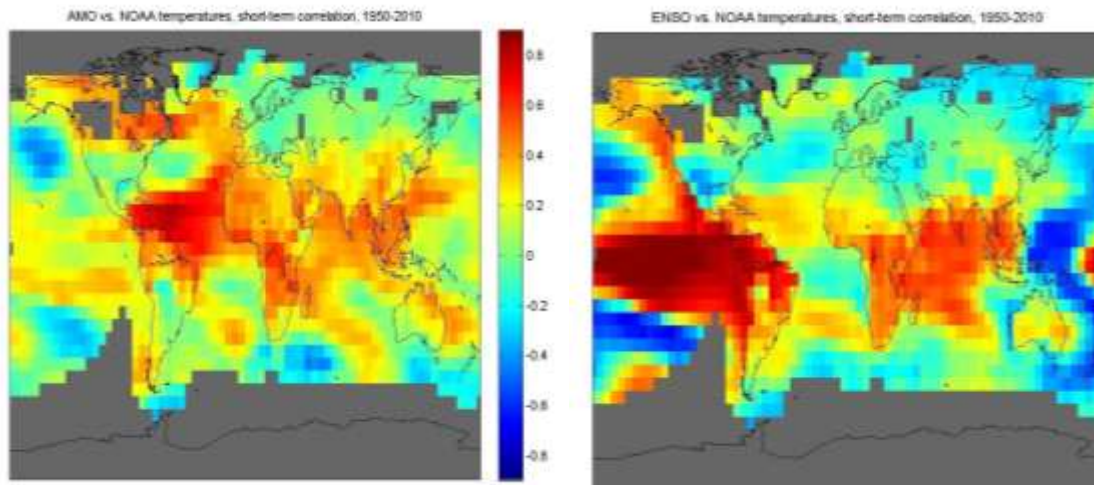

Figure 6. Correlation maps of the filtered AMO and ENSO time series with similarly filtered temperature time series taken from the Earth's surface temperature map constructed by the NOAA group. Colors show the degree of correlation at each location. AMO is observed to have positive or neutral correlation almost everywhere, while ENSO shows both strong positive and negative correlations.

Remarkably, neither AMO nor ENSO shows a strong correlation with the temperature in the United States, although ENSO reaches strongly up the west coast of the US. The variations in the Caribbean, related to the hurricane intensity hitting the southern coast of the US, is more strongly affected by AMO than by ENSO. The correlation patterns help to explain the larger association observed between AMO and Tavg than between ENSO and Tavg. ENSO is locally a more intense effect, but it is also a more complex one giving rise to both correlated and anti-correlated behavior. By contrast, the AMO map shows positive (or neutral) correlation nearly everywhere. Given this, it is not surprising that the simpler AMO association corresponds to a clearer imprint on the large scale average, Tavg.

5. Spectral Analysis

In Figure 7 we show the spectral power for the AMO and PDO pre-whitened indices. This spectral power estimate is a periodogram, calculated using a Fourier transform with no taper, padded with zeros to yield intermediate frequencies; the spectral method is described in Muller and MacDonald [2002].
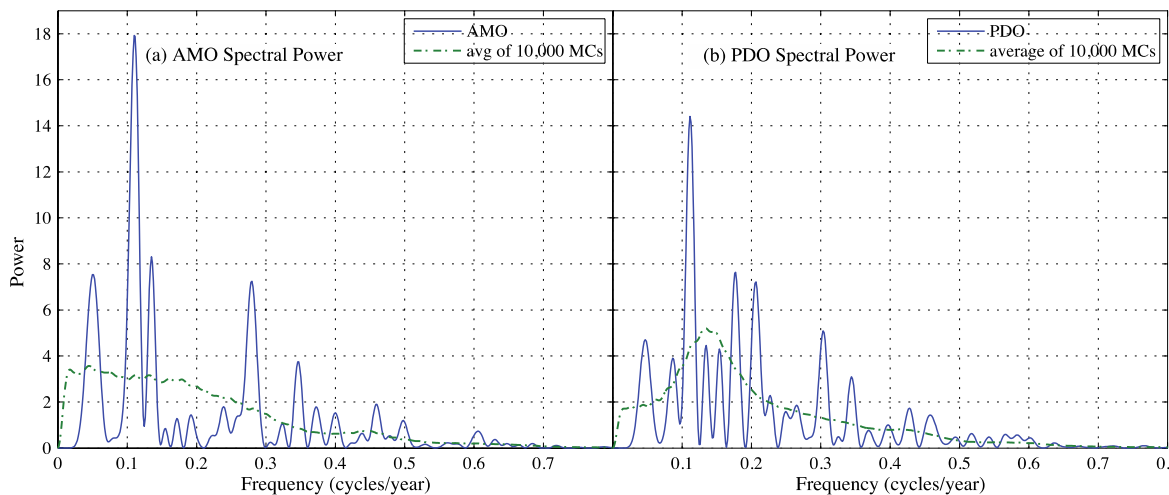
Figure 7. Spectral power in the (a) Atlantic Multidecadal Oscillation and in (b) the Pacific Decadal Oscillation. The low frequency oscillations (< 0.06/yr) have been suppressed by the subtraction of a best-fit 5th order polynomial from each time series prior to calculation of the spectrum; similarly, a 12-month running average eliminated high frequency (e.g. monthly) fluctuations. A strong peak is observed in the AMO at 0.110 ± 0.005 cycles/year, corresponding to a period of 9.1 ± 0.4 years, at the 98.3% confidence level. The maximum peak in the PDO occurs at a similar frequency, 0.111 ± 0.006, although with a confidence level of 94%.

In the AMO spectrum, a strong peak appears at frequency 0.11 ± 0.005 /yr, period 9.1 ± 0.4 years. We place no error bars on this plot because the expected distribution for a power spectrum is exponential, not gaussian. Instead, we estimate the statistical significance of this peak using the Monte Carlo approach described earlier. 10,000 time-scrambled AMO data were used as estimates of random background. In these runs, we obtained a peak (at any frequency) of spectral power level of 18 or greater a total of 170 times. Based on this, we conclude that probability that the observed peak in the unscrambled data could be due to chance is 170/10,000, i.e. the p-value is 1.7%. For the frequency uncertainty, a cycle of fixed frequency 0.1 cycle/yr and power amplitude 18 (same as the observed peak) was injected into a set of 10,000 scrambled AMO sets, and the observed root-mean-square of the frequency distribution was taken to be the frequency uncertainty.

Although the 9.1 year peak in the AMO has high statistical significance, it contains only 30% of the spectral power; for this reason its presence is not evident to the eye in Figures 3 or 4.

The highest peak in the PDO spectrum, Figure 7 (b) has period 9.0 ± 0.5 years with amplitude 14.4 and p-value 6%. None of the other peaks in Figure 6 are statistically significant. We also looked at the spectra of ENSO, NAO, and Tavg; we did not find any statistically significant narrow spectral signals, although there is of course broad power in the decadal bands.

6. Summary and Discussion

The similarity between the decadal fluctuations in land surface temperature records that use different sources indicates that the fluctuations are physical and not the effect of statistical fluctuations. The 2-15 year variations in AMO, based on sea surface temperature records, strongly correlates with the land record Tavg. Although short-term excursions, such as the temperature maximum in 1998 was widely associated with a strong El Nino event, the AMO is more closely associated with variability in the globally-average land surface temperature than is ENSO.

For a discussion of the variability of the AMO, see Frankcombe et al. [2009], who identified important variability in two time scales: 20-30 years, and 50-70 years. In this and much of other analyses prior to ours, the key focus was on longer time scales and so the data were smoothed with a decade-long running average; such a procedure suppresses the interannual to decadal scale variations (2 to 15 year) that are the subject of the present paper.
In the interannual to decadal region we studied, there is only one statistically-significant spectral peak, with the period of 9.1 ± 0.4 years, strong in the AMO, weaker in the PDO. It is not present at a statistically significant level in the land Tavg or in ENSO or in other ocean indices that we examined. Spectral analysis of global temperatures by others had previously yielded claims of many frequencies, most of which we conclude are not statistically significant when we analyze them using our Monte Carlo background estimation. For example, Scafetta [2010], reported a forest of 11 spectral peaks based on a multitaper analysis; to each of these peaks he calculated 99% confidence intervals. He reported 7 peaks with periods in the range from 5.99 years to 14.8 years. One of these is at our period of 9.1 years; he suggests that this year cycle could be induced by lunar tidal variations. However, we find that when we use our Monte Carlo methods to estimate background, none of his claimed peaks are statistically significant except for the 9.1 year peak; we do not find them in the AMO, PDO, or ENSO.

Correlation does not imply causation. The association between Atlantic sea surface temperature fluctuations and land temperature may simply indicate that both sets of temperatures are responding to the same source of natural variability. However, it is also interesting to consider whether oceanic changes in the AMO may be driving short-term fluctuations in land surface temperature. Such fluctuations might originate as instabilities in the AMO region itself, or they might occur as a non-linear response to changes elsewhere (such as within the ENSO region).

If the fluctuations originate locally, then they might be associated with natural variations in the meridional overturning circulation (MOC) or from salinity anomaly events (Dickson et al., 1988; Belkin,2004). They could be related to a larger instability in the flow of the thermohaline circulation (the oceanic conveyor belt). Computer simulations of the thermohaline circulation by Jungclaus et al. [2010] "show pronounced multidecadal fluctuations of the Atlantic overturning circulation and the associated meridional heat transport. The period of the oscillations is about 70–80 yr. The low-frequency variability of the meridional overturning circulation (MOC)

contributes substantially to sea surface temperature and sea ice fluctuations in the North Atlantic."

A theory for decadal oscillations in the North Pacific was devised by Munnich [1998]. It involves an interaction between wind and the thermohaline circulation. Such models predict broad spectrum of frequencies, and could drive the structure we see in Figure 3(A), but we would not expect such a driving force to result in the narrow 9.1 yr peak. For more on exited internal modes, see Frankcombe et al. [2010] and Sévellec et al. [2009, 2010] and the references therein.

Given that the 2-15 year variations in world temperature are so closely linked to the AMO raises (or re-raises) an important ancillary issue: to what extent does the 65-70 year cycle in AMO contribute to the global average temperature change? (Enfield, 2006; Zhang et al., 2007; Kerr, 1984.) Since 1975, the AMO has shown a gradual but steady rise from -0.35 C to +0.2 C (see Figure 2), a change of 0.55 C. During this same time, the land-average temperature has increased about 0.8 C. Such changes may be independent responses to a common forcing (e.g. greenhouse gases); however, it is also possible that some of the land warming is a direct response to changes in the AMO region. If the long-term AMO changes have been driven by greenhouse gases then the AMO region may serve as a positive feedback that amplifies the effect of greenhouse gas forcing over land. On the other hand, some of the long-term change in the AMO could be driven by natural variability, e.g. fluctuations in thermohaline flow. In that case the human component of global warming may be somewhat overestimated.

In conclusion, our analysis suggests that strong interannual and decadal variations observed in the average land surface temperature records represent a true climate phenomenon, not only during the years when fluctuations on the timescale of 2-15 years had been previously identified with El Nino events. The variations are strongly correlated with the similar decadal fluctuations observed in the Atlantic Multidecadal Oscillation index, and less so with the El Nino Southern Oscillation index. This correlation could indicate that the AMO plays an important intermediary role in the influence of the Pacific ENSO on world climate; alternatively, it might indicate that variability in the thermohaline flow plays a bigger role than had previously been recognized. The models could be tested by studying the temperature correlations in the ocean as a function of location and time. A 9.1 ± 0.4 year cycle is observed in the pre-whitened AMO, but it contributes only 30% to the variance. A similar cycle at 9.0 ± 0.5 years is seen in the PDO.

7. Acknowledgments

8. References

[1] Belkin, I.M. (2004), Propagation of the "Great Salinity Anomaly" of the 1990s around the northern North Atlantic. Geophys. Res. Lett., 31, L08306.

[2] Brohan, P., J. J. Kennedy, I. Harris, S. F. B. Tett & P. D. Jones (2005), Uncertainty estimates in regional and global observed temperature changes: a new dataset from 1850, J. Geophys. Res. 111, D12106, soi:10.1029/2005JD006548. Temperature data are available at:
http://hadobs.metoffice.com/hadcrut3/diagnostics/comparison.html

[3] Dickson, R. R., Meincke, J., Malmber, S. A. & Lee, A. J. (1988), The ''great salinity anomaly'' in the northern North Atlantic 1968–1982. Prog. Oceanogr. 20, 103–151. Enfield, D.B., A.M. Mestas-Nunez, and P.J. Trimble (2001), The Atlantic Multidecadal Oscillation and its relationship to rainfall and river flows in the continental U.S., Geophys. Res. Lett., 28: 2077-2080.

[4] Frankcombe, L. M., A. von der Heydt and H. A. Dijkstra (2010) North Atlantic Multidecadal Climate Variability: An investigation of dominant time scales and processes, J. Climate, 23, 3626–3638, available at
www.phys.uu.nl/~heydt/Publications/Frankcombe-etal-2010.pdf

[5] Hansen, J., R. Ruedy, Mki. Sato, and K. Lo (2010), Global surface temperature change. Rev. Geophys., 48, RG4004, doi:10.1029/2010RG000345. Updated Land Temperature data available at: data.giss.nasa.gov/gistemp/graphs/

[6] Hurrell, J.W., (1995) Decadal trends in the North Atlantic Oscillation and relationships to regional temperature and precipitation. Science 269, 676-679.

[7] Jones, P.D., Jónsson, T. and Wheeler, D. (1997), Extension to the North Atlantic Oscillation using early instrumental pressure observations from Gibraltar and South-West Iceland. Int. J. Climatol. 17, 1433-1450. The NAO index data are available from NCAR at www.cgd.ucar.edu/cas/catalog/climind/

[8] Jones, P. D., and A. Moberg (2003), Hemispheric and Large- Scale Surface Air Temperature Variations: An Extensive Revision and an Update to 2001, J. Clim., 16, 206–23;

[9] Jungclaus, J. H., H. Haak, M. Latif, U. Mikolajewicz (2005), Arctic–North Atlantic Interactions and Multidecadal Variability of the Meridional Overturning Circulation, J. Clim., pp. 4013-4030.

[10] Kerr, R. A., A North Atlantic Climate Pacemaker for the Centuries (2000), Science 16 Vol. 288 no. 5473 pp. 1984-1985. DOI: 10.1126/science.288.5473.1984 Meehl, Gerald A., W.M. Washington, C. M. Ammann, J. M. Arblaster, T. M. L. Wigley, C. Tebaldi (2004). "Combinations of Natural and Anthropogenic Forcings in Twentieth-Century Climate". J. Clim. 17: 3721–7. DOI:10.1175/1520-0442(2004)017%3C3721:CONAAF%3E2.0.CO;2. ISSN 1520-0442.

[11] Menne, M.J., and C. N. Williams (2005), Detection of undocumented change points using multiple test statistics and reference series, J. Clim., 18, 4271-4286.   The NOAA average land temperature estimate can be downloaded at ftp.ncdc.noaa.gov/pub/data/anomalies/monthly.land.90S.90N.df_1901-2000mean.dat

[12] Muller, R. A. and G. MacDonald, (2002), Ice Ages and Astronomical Causes: data, spectral analysis, and models. 337 p. ISBN 978-3540437796. Springer/Praxis Publishing.

[13] Munnich, M. Latif, S. Venzke, E. Maier-Reimer (1998), Decadal Oscillations in a Simple Coupled Model, J. Clim. vol 11, 3309-3319.

[14] NOAA (2011). We used the Nino 3.4 data available from the Earth System Research Laboratory, Physical Sciences Division, at: www.esrl.noaa.gov/psd/data/correlation/nina34.data and from the NOAA Climate Prediction Center at: www.cpc.ncep.noaa.gov/data/indices/wksst.for

[15] Rohde, R., D. Brillinger, J. Curry, D. Groom, R. Jacobsen, R.A. Muller, S. Perlmutter, A. Rosenfeld, C. Wickham, J. Wurtele (2011), Berkeley Earth Temperature Averaging Process, submitted to Econometrics.

[16] Scafetta, N. (2010), Empirical evidence for a celestial origin of the climate oscillations and its implications. Journal of Atmospheric and Solar-Terrestrial Physics, doi:10.1016/j.jastp.2010.04.015 Schlesinger, M. E., and Ramankutty, N. (1994), An Oscillation in the global climate system of period 65-70 years, Nature 367, 723 - 726); doi:10.1038/367723a0

[17] Sévellec, F. and A. V. Fedorov (2010), Excitation of SST anomalies in the eastern equatorial Pacific by oceanic optimal perturbations, accepted in J. Mar. Res.

[18] Sévellec, F., T. Huck, M. Ben Jelloul and J. Vialard (2009), Non-normal multidecadal response of the thermohaline circulation induced by optimal surface salinity perturbations, J. Phys. Oceanogr., 39, 852-872.

[19] Thompson, D. W. J., and J. M. Wallace (1998), The Arctic Oscillation signature in the wintertime geopotential height and temperature fields. Geophys. Res. Lett., 25, No. 9, 1297-130.

[20] Trenberth, K.E., J. M. Caron, D. P. Stepaniak, and S. Worley (2002), Evolution of El Niño–Southern Oscillation and global atmospheric surface temperatures   J.Geophys.Res., 107, D8, doi:10.1029/2000JD000298, 2002

[21] Trenberth & Shea (2006), Geophysical Research Letters 33, L12704, doi:10.1029/2006GL026894. Updated index available from NOAA at: www.esrl.noaa.gov/psd/data/correlation/amon.us.long.data and www.cdc.noaa.gov/Timeseries/AMO/

[22] Zhang, R., and T. L. Delworth (2007), Impact of the Atlantic Multidecadal Oscillation on North Pacific climate variability. Geophysical Research Letters, 34, L23708, doi:10.1029/2007GL031601.

[23] Zhang, R., T. L. Delworth, and I. Held (2007), Can the Atlantic Ocean drive the observed multidecadal variability in Northern Hemisphere mean temperature? Geophysical Research Letters, 34, L02709, doi:10.1029/2006GL028683